Histol Histopathol (2003) 18: 359-369

http://www.hh.um.es

Histology and Histopathology

Cellular and Molecular Biology

Altered Cx43 expression during myocardial adaptation to acute and chronic volume overloading

L. Formigli[1], L. Ibba-Manneschi[1], A.M. Perna[2], A. Pacini[1], L. Polidori[1], C. Nediani[3], P.A. Modesti[4], D. Nosi[1], A. Tani[1], A. Celli[3], G.G. Neri-Serneri[4], F. Quercioli[5] and S. Zecchi-Orlandini[1]

Departments of [1]Anatomy, Histology, Forensic Medicine, [3]Biochemical Sciences, [4]Internal Medicine and Cardiology, University of Florence, [2]Department of Experimental Cardiology, Careggi Hospital and [5]National Institute of Applied Optics, Laboratory of Bio-Photonics, Florence, Italy

Summary. Gap-junctions are specialized regions of intercellular contacts allowing electrical impulse propagation among adjacent cardiomyocytes. Connexin43 (Cx43) is the predominant gap-junction protein in the working ventricular myocardium and its reduced expression has been extensively implicated in the genesis of conduction abnormalities and re-entry arrhythmia of chronically hypertrophied hearts. In contrast, data on the role played by this protein during cardiac remodeling and early phases of developing hypertrophy are lacking. Therefore, in the present study, we investigated this issue using an experimental model of pig left ventricle (LV) volume overloading consisting in the creation of an aorto-cava fistula. At scheduled times (6, 24, 48, 96, 168 h, and 2, 3 months after surgery) echocardiographic and haemodynamic measurements were performed and myocardial biopsies were taken for the morphological and biochemical analyses. When faced with the increased load, pig myocardium underwent an initial period (from 6 up to 48 h) of remarkable tissue remodeling consisting in the occurrence of cardiomyocyte damage and apoptosis. After that time, the tissue developed a hypertrophic response that was associated with early dynamic changes (up-regulation) in Cx43 protein expression, as demonstrated by Western blot and confocal immunofluorescence analyses. However, an initial transient increase of this protein was also found after 6 h from surgery. With the progression of LV hypertrophy (from 168 hr up to 3 months), a reduction in the myocardial Cx43 expression was, instead, observed. The increased expression of Cx43 protein during acute hypertrophic response was associated with a corresponding increase in the levels of its specific mRNA, as detected by RT-PCR. We concluded that up-regulation of Cx43 gap-junction protein could represent an immediate compensatory response to support the new working conditions in the early stages of ventricular overloading.

Key words: Connexin43, volume-overload, pig myocardium, hypertrophy, confocal microscopy.

Offprint requests to: Prof. S. Zecchi-Orlandini Department of Anatomy, Histology, Forensic Medicine, Viale Morgagni 85, 50134 Florence, Italy. Fax: +39 055 4379500. e-mail: zecchi@unifi.it

Introduction

It is well known that ventricular hypertrophy represents a fundamental adaptive response of the heart to the increased working demand (Chien, 1999). In response to biomechanical stress, such as chronic pressure overloading (i.e. long-lasting hypertension) and volume overloading (i.e. post-myocardial injuries) the heart, in fact, initiates a process leading to the increase in cardiac mass and augmentation of the pump function (Anversa and Capasso, 1991). The expansion of myofibrillar apparatus of cardiomyocytes and collagen deposition occurring during hypertrophy (Mercadier et al., 1981) results from the interaction between mechanical stresses (i.e. external load) and the release of autocrine/paracrine growth factors, such as Angiotensin II (AngII), Endothelin 1 (ET-1) and Insulin-like Growth Factor-I (IGF-I) (Baker et al., 1990; Modesti et al., 2000; Molkentin, 2000). Although initially beneficial, sustained cardiac hypertrophy may incur a temporal deterioration leading to the impairment of the cardiac function and heart failure (Chien, 1999; Minamisawa et al., 1999). A substantial number of reports in the literature regards the pathological mechanisms underlying the ventricular dysfunctions associated with hearts in advanced stage of hypertrophy. In contrast, little is known about the adaptive processes involved in the early phases of ventricular overloading and during developing cardiac hypertrophy. Remodeling of intercellular junctions among cardiomyocytes in diseased myocardium may well represent one of these mechanisms. Indeed, gap-junction channels, which are predominantly formed by Cx43 protein in the working ventricular myocardium, provide a pathway for the

intercellular exchange of metabolite and ions necessary for potential coordinated action propagation among adjacent cardiomyocytes (Saffitz, 1997; Yeager, 1998). In fact, reduced expression of myocardial Cx43 protein, has been related to abnormalities in the intercellular propagation of the electrical impulse (Saffitz et al., 1999; Beardslee et al., 2000) and, in turn, to the following mechanical deficiencies observed in hearts under hypertensive conditions (Uzzaman et al., 2000; Emdad et al., 2001) and in human hypertrophied and/or congestive heart failure (Peters et al, 1993; Peters, 1996; Dupont et al., 2001; Severs et al., 2001). However, only a few "in vitro" studies have postulated an involvement of this protein in the development of the immediate adaptive hypertrophic response. In particular, early modulators of heart hypertrophy, such as cAMP and ANG II (Darrow et al., 1996; Dodge et al., 1998), as well as 1 to 4 hours of pulsatile stretches (Zhuang et al., 2000) have been shown to induce in cultured cardiomyocytes a rapid up-regulation of Cx43 protein associated with a marked increase in impulse propagation velocity. Thus, it appears from the above reported findings, that modifications in the ventricular Cx43 protein expression may be dependent on the duration of the application of the increased ventricular workload. To address just this issue, we investigated in the present study, the "in vivo" distribution of Cx43 protein during development and progression of left ventricle (LV) hypertrophy in a model of volume-overload hypertrophy in the pig. Confocal laser scanning microscopy and Western blot were used to evaluate changes in Cx43 expression at the protein level, whereas RT-PCR was used to correlate the expression of the protein to that of its specific mRNA.

Materials and methods

Surgical protocol

Thirty-two farm pigs aged 2-3 months, weighing 35-40 Kg, were enrolled in this study. The animals were kept and handled according to the standards detailed in the Guide for the Care and Use of Laboratory Animals published by the U.S. National Institute of Health (NIH Publication No. 85-23, revised 1996). The animals were randomly divided into two groups: a group of sham-operated (controls) (n=4) and a group (n=28) with aorto-cava shunt. At each set experimental time (6, 24, 48, 96, 168 h and 2 and 3 months after surgery) four animals underwent haemodynamic measurements before the sacrifice. Regarding the surgical protocol, all the animals were premedicated with intramuscular Ketamine (15 mg/kg) and Diazepam (5mg/kg). Anesthesia was induced with pentobarbital sodium (20 mg/kg iv) and maintained by inhalation of a mixture of 1-1,5% fluothane and O_2 supplemented with bromide pancuronium (0.1 mg/kg) and Ketamine. Peripheral electrocardiography leads were tied. Femoral vessels were exposed and cannulated for haemodynamic measurements. To induce myocardial volume overload, the abdomen was opened via midline incision, and the inferior vena cava and abdominal aorta were dissected free from surrounding tissues distally to the renal arteries. A side clamp was used after systemic heparinization (3mg/kg) and a Dacron graft (8 μm diameter) was inserted between the aorta and the vena cava by means of a continuous running suture. The clamp was then released and the abdomen closed. Sham-operated animals underwent laparotomy, medication and haemodynamic evaluations in the same way as experimental animals. At each experimental time, the heart was removed by a midline sternotomy and small transmural fragments from the anterior wall of the left ventricle were either frozen in liquid nitrogen or fixed in 4% buffered paraformaldehyde and 2.5% glutharaldehyde for light microscopic and transmission electron microscopic analysis respectively.

Left ventricular function and haemodynamic measurements

Two 6F pigtail catheters were introduced into the left femoral artery and advanced to monitor left ventricular pressure and descending aortic pressure simultaneously. A Swan-Ganz catheter was advanced from an external jugular vein to the pulmonary artery to measure pulmonary arterial pressure and cardiac output (thermodilution). Two-dimensional and M-mode echocardiographic studies (2.25/3.5-Mhz transducer, SIM 5000) were performed from the right parasternal area, and the studies were recorded on videotape. Freeze-frames were printed and wall thickness and left ventricular diastolic internal dimensions were measured according to the recommendations of the American Society of Echocardiography. Left ventricular mass (LVM) was calculated using validated formulas as previously reported (Devereux and Reichek, 1997; Modesti et al., 2000; Neri Serneri et al., 2000) and normalized for body weight. End-systolic stress (ESS) was calculated from echocardiographic recordings in combination with invasive left ventricular pressure. Measurements were analysed independently by two experienced echocardiographers. Inter-observer and intra-observer variability were 4.1±0.5% and 2.5±0.3% for cavity size and 3.7±0.4% and 2.1±0.3% for wall thickness, respectively.

Ultrastructural analyses

For transmission electron microscopy (TEM), small tissue samples from control and volume-overloaded myocardium were fixed in 4% glutaraldehyde in 0.1 M sodium cacodylate buffer, pH7.4, for 3 hours at room temperature, and postfixed in 1% osmium tetroxide in 0.1 M phosphate buffer, pH7.4, for 1 hour at 4 °C. They were then dehydrated in graded acetone, passed through propylene oxide and embedded in Epon 812. Ultrathin sections were stained with uranyl acetate and alkaline

bismuth and viewed under a JEM 1010 electron microscope (Jeol, Tokyo, Japan) at 80 kV.

Detection of apoptotic cells

In situ end labeling of nicked DNA (ISEL assay) was performed on paraffin-embedded sections from control and volume-overloaded myocardium as previously reported (Wijsman et al., 1993) with minor modifications. Briefly, after a treatment with 20% g/ml protease K to remove the excess protein from nuclei, the tissue sections were incubated with the Klenow fragment of DNA polymerase I and biotylinated deoxynucleotides (FRAGEL-Klenow, DNA fragmentation kit, Calbiochem, CA) in a humidified chamber at 37 °C for 1.5 h. After that, the sections were incubated with streptoavidin-peroxidase for 10 min and then stained with diaminobenzidine tetrahydrochloride (DAB). Counterstaining was performed with methyl green. Apoptotic nuclei were easily recognized by the presence of a dark brown staining in contrast with that of necrotic and mitotic cells which instead appeared weakly stained. Viable cells appeared green. The number of apoptotic cardiomyocytes in ISEL-stained sections was counted by the use of an LM with an ocular grid (area of the field = 26,300 μm^2) at x40. An average of 384 microscopic fields (four in each section for a total of three sections for each biopsy examined) were analyzed by two different observers and the individual values were then averaged. The reported data are expressed as ± SD of means. Comparison between different groups was performed by ANOVA followed by Bonferroni t-test. A value of $p<0.05$ was accepted as statistically significant.

Measurement of interstitial fibrosis

After fixation in formalin, the myocardial samples were dehydrated and embedded in paraffin. Longitudinal sections, 6 μm thick, were routinely stained with Masson's trichrome modified by Goldner (Bio-Optica, Milan, Italy) to specifically identify collagen fibers. Interstitial fibrosis, from which perivascular collagen was excluded, was determined in 6 randomly selected fields from each tissue section (for a total of three sections for each biopsy examined). A total number of 576 optical fields of 24,4000 μm^2 each was collected at x20. The images were collected by Adobe Photoshop 5.0 and elaborated using the Scion Image Program. Quantitative analyses were performed on the number of pixels corresponding to fibrosis in each optical field, and the data were expressed in μm^2 .

Measurement of cell size

Additional semithin sections were stained with 1% Toluidine-blue. At each experimental time, 10 myocytes from 6 randomly selected optical fields in each transversely sectioned specimens (3 from each animal) of 26,300 μm^2 were analyzed at a magnification of x40 by Adobe Photoshop Program. The area of individual cells containing well defined round nuclei were measured using the Scion Image Program.

Western blot analysis of connexin43 and densitometry.

After mechanical pulverization in liquid nitrogen, total proteins from left ventricle specimens, which were kept at -80 °C until use, were extracted in lysis buffer (10 mM Tris-HCl [pH 7.4], 0.1% sodium dodecyl sulfate (SDS) 1 mM phenylmethanesulfonyl fluoride, 1 μg/ml leupeptin, 1 μg/ml aprotinin) by homogenization and incubated at 95 °C for 15 minutes. Protein concentration was measured by the Bio-Rad protein assay. Each sample of 20 μg total proteins was denaturated by heating to 95°C in electrophoresis buffer (125 mM Tris-HCl [pH 6.8], 20%, glycerol, 4% SDS, 10% ß-mercaptoethanol and 0.1% bromophenol blue), and loaded onto a 15% SDS polyacrylamide gel. Protein transfer to polyvinylidene fluoride membranes (PVDF, Amersham) was performed (Hoefer Transphor unit) for 1 h at 100 volts. Transfer efficiency was verified by total protein staining of the gels with Coomassie blue. Membranes were incubated with 4 μg/ml of monoclonal (mouse) anti-connexin-43 antibody (Chemicon International Inc.) at room temperature for 2 h. Blots were washed with T-TBS (Tris 50 mM [pH 7.5], NaCl 0.15 mM, Tween 0.1%) and incubated with peroxidase-conjugated anti IgG mouse antibody (Amersham). For detection of antibody binding an enhanced chemiluminescence assay was used (Supersignal West-Dura; Pierce). Signals were quantified using the program for image analysis and densitometry Quantity One (Biorad). The data from densitometric analysis were related to the amount of protein used on the PAGE and were not significantly altered when these values were related to ß–MHC protein levels. Quantitative data are expressed as percentage of control value.

Confocal Cx43 immunostaining and quantitative analysis

Immunostaining for Cx43 protein was carried out on 6 μm-thick cryosections. Prior to incubation with the specific antibody, the sections were incubated with PBS containing 3% BSA and gelatin to reduce non-specific staining. Cx43 MoAb (Chemicon International Inc., CA) was then added at 1:40 dilution overnight at 4 °C. After removal of unbound antibodies, the immunoreactivity was detected with Alexa-488-conjugated secondary Ab (Molecular Probes, Eugene, OR). Counterstaining for F actin was also performed using rhodamine-phalloidin (Sigma, St. Louis, MO). Anti-fading glycerol was used as mounting medium. A Bio-Rad confocal microscope (MCR 1024-ES) equipped with a 15mW Krypton/Argon laser source was used to collect images. Dual channel scanning of signals from actin (red) and Cx43 (green) were recorded separately to avoid bleedthrough, and were saved in two different files. Images were signal-averaged during acquisition by using the Kalman

averaging option (5 scans) to reduce noise level and improve the quality of the image. For the quantitative evaluation of Cx43, the immunolabeling procedures, image acquisition and analyses were performed under identical conditions. No image processing after acquisition was performed in order to minimize errors. Eight sections from sham-operated and volume-overloaded pig hearts (taken at 48, 96, 168 hours and 2 and 3 months) were analyzed. For each section, a randomly chosen optical field (170x170mm) was selected. Series of confocal optical sections (512x512 pixels) were then taken throughout the depth of the specimens (10 μm) with a thickness of 1mm at intervals of 0.5 μm, by using a Nikon planapo x60 1.4 oil immersion objective. Fifteen optical sections for each set of samples were then projected as single composite images by superimposition. An arbitrary threshold for each image was calculated by the use of the formula: T= m+3d, where m is the mean intensity value and d is the standard deviation (SD). The so-identified signal threshold corresponded to a value that best distinguished connexin staining from the surrounding background. Connexin43 expression was then quantified as the number of pixels exceeding the threshold that were proportional to the tissue area occupied by the gap-junctional protein, normalized to the total tissue area (actin staining), as previously described (Saffitz et al., 2000a).

Semiquantitative RT-PCR

For the quantification of Cx43 mRNA levels, total RNA was extracted by homogenization in 1 ml of TriReagent (Sigma, St. Louis, MO) according to the manufacturer's protocol. Semiquantitative determination of Cx43 mRNA levels was done by an internal standard-based PCR assay using GAPDH as reference gene. A 288-bp segment on the pig Cx 43 cDNA sequence (GenBank™ accession number X86023) was targeted with upstream primer 5'-TACCACGCCACCACCG-3', and downstream primer 5'-TTGGCTGTCGTCAGGGA AAAT-3', while a 346-bp segment of the pig GAPDH sequence was amplified with upstream primer 5'-ACCCAGAAGACTGTGGATGG-3', and downstream primer 5'-CCCCAGCATCAAAGGTAGAA-3'. 200 ng of total RNA was reverse-transcribed with SuperScript™ One-Step™ RT-PCR System (Invitrogen, Groningen, The Netherlands) in a total volume of 50 μl. After cDNA synthesis for 30 min at 55 °C the samples were pre-denatured for 2 min at 92°C; the first-strand cDNA was subjected to 35 cycles of PCR performed at 94 °C for 15 sec, 55°C for 30 sec, and 72 °C for 1 min; the final extension step was performed at 72 °C for 5 min. Internal standards for quantification of Cx43 cDNA were generated by amplifying GAPDH mRNA using the same PCR program. Amplification products were run on a 1.8% agarose gel and the ethidium bromide-stained bands were quantitated by densitometric analysis. The mRNA levels at different time points were calculated as ratios of Cx43 to GAPDH.

Statistical analysis

All data are reported as mean ± SD. Comparison among different groups was performed by ANOVA followed by Bonferroni t-test. A value of $p<0.05$ was accepted as statistically significant.

Results

Haemodynamic and echocardiographic data

During the whole period of the experimentation, the shunt remained patent in all the operated pigs and no animal died or showed ouvert signs of heart failure. The haemodynamic and transthoracic echocardiographic values are reported in Table 1. The trend of the recorded parameters suggested that cardiac function was progressively impaired reaching its peack at 48 h from surgery as shown by the behavior of right ventricular and

Table 1. Echocardiographic and haemodynamic measurements of sham-operated (controls) and hypertrophied pig hearts.

	CONTROLS	6 h	24 h	48 h	96 h	168h	2 m	3 m
H.R. (Beats/min)	82±5	116±4*	111±8*	108±8*	107±7*	108±7*	100±9*	95±3*
A.P. (mmHg-systolic)	125±18	113±7*	115±4*	116±7	117±4	116±6	120±7	116±4
R.V.P. (mmHg-mean)	27±5	42±7*	50±4*	52±6*	50±7*	49±5*	45±7*	42±4*
P.W.P. (mmHg-mean)	14±4	22±5	23±4*	25±5*	21±4*	22±7*	20±3*	19±2*
C.O. (ml/min)	2009±463	3213±417*	3549±888*	3370±503*	3519±203*	3905±878*	3100±327*	3005±421*
L.V.E.S.P.(mmHg)	127±23	121±5	121±11	123±5	124±7	127±15	131±12	134±4
L.V.E.D.P(mmHg)	8±2	15±1*	14±2*	12±2*	11±1*	10±2	9±7	9±5
S.W.T.(mm)	11.2±1	10.9±0.9	11.1±0.3	11.1±1.2	11.4±1.1	11.5±0.5	11.8±0.9	11.9±0.3
D.W.T.(mm)	7.8±0.7	7.4±0.5	8.0±0.9	7.9±0.8	8.1±0.6	8.1±0.4	8.7±0.5	8.9±0.5
E.S.S.(Kdyne cm^2)	47±5	45±3	45±5	47±2	46±4	48±3	55±2	61±3*
L.V.M.	2.69±0.54	2.72±0.47	2.71±0.61	3.01±0.90	3.15±0.44*	3.71±0.28*	4.54±0.57*	6.08±0.32*

H.R.: heart rate; A.P.: aortic pressure; R.V.P.: right ventricular pressure; P.W.P.: pulmonary wedge pressure; C.O.: cardiac output; L.V.E.S.P.: left ventricular end systolic pressure; L.V.E.D.P.: left ventricular end diastolic pressure; S.W.T.: systolic wall thickness; D.W.T.: diastolic wall thickness; E.S.S. end systolic stress; L.V.M.: left ventricular mass. Values are meean ± SD. +: $p<0.05$ vs baseline.

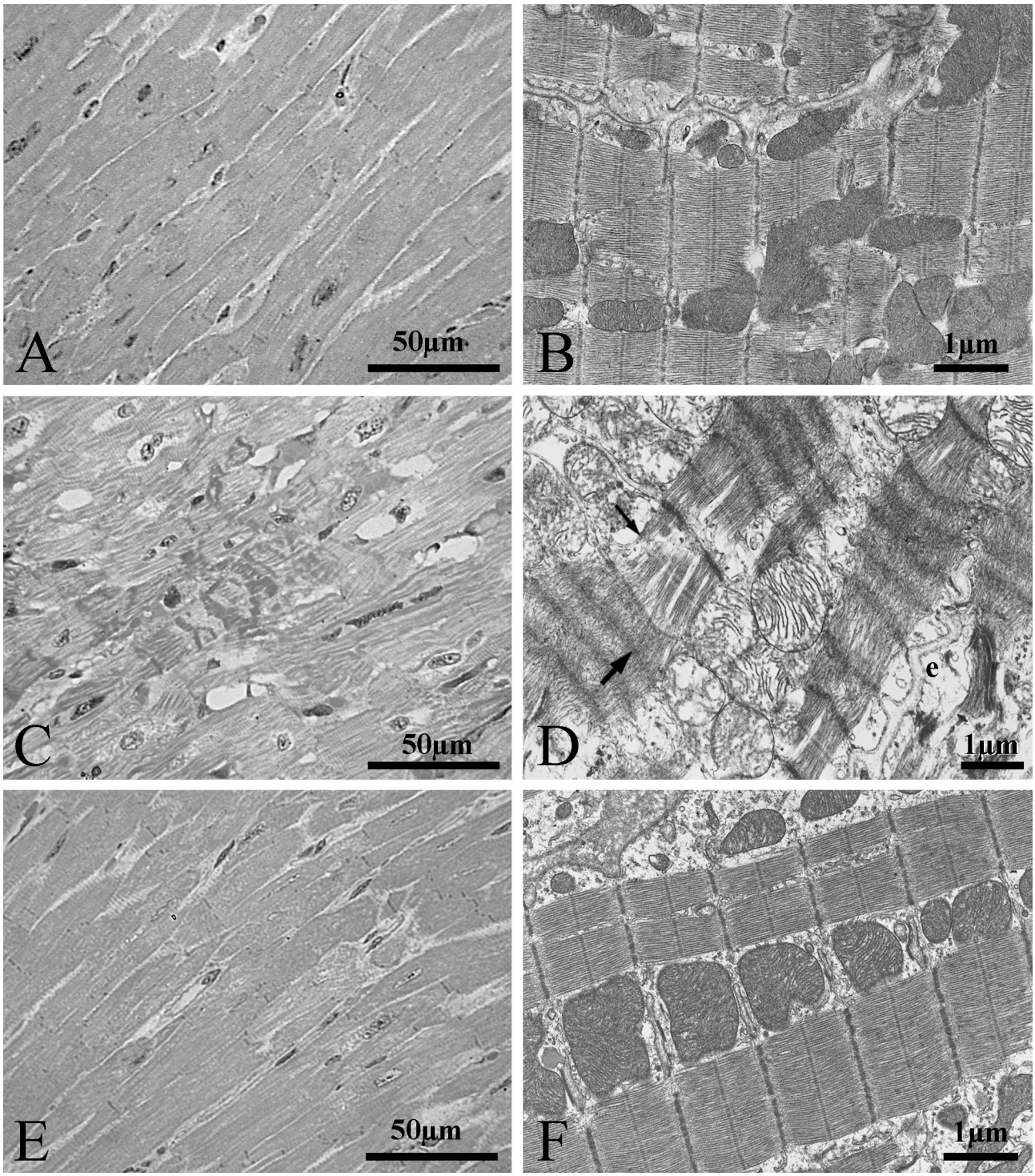

Fig. 1. Light and transmission electron micrographs of sham operated (control) **(A, B)**, 6 h **(C, D)** and 168 h **(E, F)** volume-overloaded myocardium. **C.** Some cardiomyocytes exhibit several contraction bands. **D.** At higher magnification, the cytoskeletal alterations consist mainly in hypercontracted sarcomeres (thick arrow) associated with overstretched myofilaments (thin arrow); note that myofibrils are interspersed with a prominent accumulation of intracellular oedema (e) and seriously damaged mitochondria. **E.** Cardiomyocytes show a normal appearance and contain regularly arranged sarcomeres and mitochondria with well preserved cristae **(F)**.

pulmonary wedge pressures as well as cardiac output. Pressure values increased rapidly after surgery reaching highest levels at 48 h whereas cardiac output, although significantly higher compared to values recorded immediately after surgery, showed a 5% drop at 48 h. No significant changes were observed in LVESP during the whole period of the experimentation; on the contrary, a significant increase in LVEDP (taken as an index inversely correlated with heart contractility) was recorded in the earliest phases (6-48 h) of volume overloading. After having achieved the maximum values at 48 h, LVEDP decreased to return to the baseline values in the following time points. These latter modifications were similar to those observed in the pulmonary wegde pressure. After 3 months, several parameters returned close to the normal values, only right heart pressures were still elevated with a cardiac output significantly higher then before shunt All echocardiographic findings were indicative of a compensatory hypertrophy of the left ventricle as shown by values of L.V.M. and E.S.S.

Morphological analysis and ultrastructure

The morphological evaluation performed by LM and TEM of LV volume-overloaded myocardium revealed the occurrence of remarkable tissue damage in the period ranging between 6 and 48 h from surgery (Fig. 1). With respect to sham-operated (control) myocardium (Fig. 1A,B) damaged cardiomyocytes showed loss of sarcomere registration and contraction bands, consistent oedema accumulation, and swelling of the intramitochondrial matrix associated with fragmentation of cristae (Fig. 1C,D). These modifications, which were focally distributed (Fig. 1C) within LV myocardium, were particularly evident around 24 and 48 h from surgery and thereafter attenuated (96 h) and disappeared almost completely after 168 h (Fig. 1E,F). At this time, in fact, cardiomyocytes appeared to be structurally similar to those of controls and their normal morphology was apparently preserved during the whole period of the hypertrophic growth. In addition to the above ultrastructural defects, signs of apoptotic degeneration could be also identified in the myocardium during the early phases of volume overloading. In fact, when "in situ" end labeling (ISEL) assay was used as an indicator of DNA fragmentation, several cardiomyocytes were shown to contain strongly positive nuclei within the first week from operation. No apoptotic nuclei in the interstitial spaces or in the endothelial lining of blood vessels were found. We calculated that the number of myocytes undergoing apoptosis increased from approximately undetectable in the control myocardium to a maximum of 34.7 in the samples subjected to 48h of LV overloading (Fig. 2A,C). Thereafter, the number of ISEL-positive nuclei decreased significantly (96 h)

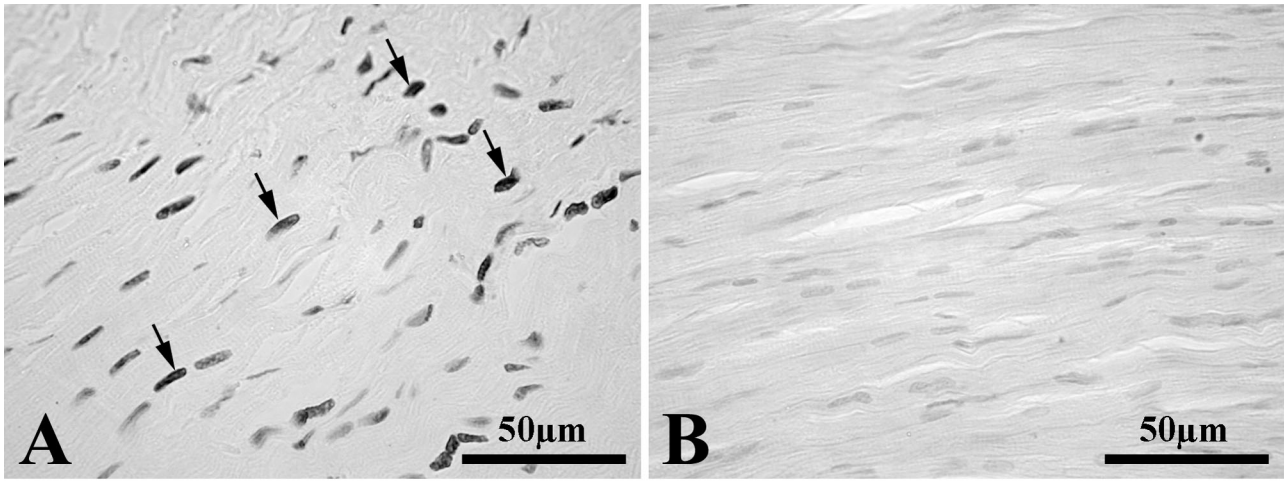

C

C	6 h	24 h	48h	96 h	168h	2 m	3 m
0.72 ±0.15	18.3±8.82	19.9±5.96	34.7±11.10	10.9±5.36	0.19±0.09	0.23±0.15	0.19 ±0.06

Fig. 2. Detection of apoptotic cells by in situ end labeling (ISEL) assay of fragmented DNA. **A.** Representative LM micrograph of 48 h-volume overloaded myocardium. Note that some cardiomyocytes (arrows) exhibit dark brown-stained ISEL-positive nuclei. **B.** LM micrograph of 168-h volume-overloaded myocardium. Virtually no cardiomyocyte stain positively for apoptotic nuclear fragmentation. **C.** Quantitative analyses of cardiomyocytes undergoing apoptosis as measured by ISEL assay. All data are statistically significant vs controls and vs each group examined except for 24 and 96 vs 6h; 3 ms vs controls 168 h and 2 ms; 2 ms vs controls and 168 h.

reaching a number similar to the control ones after 168 h which remained practically unchanged during the whole period (Fig. 2B,C). The latter findings suggested that a true apoptotic wave characterized the initial period of myocardial remodeling observed in our experimental conditions.

The application of LV-volume overloading induced a significant increase in myocyte cross-sectional areas which was associated with an increase, although to a lesser extent, in the interstitial collagen content in the myocardium from pigs with aorto-cava fistula as compared with that of sham-operated controls (Fig. 3A,

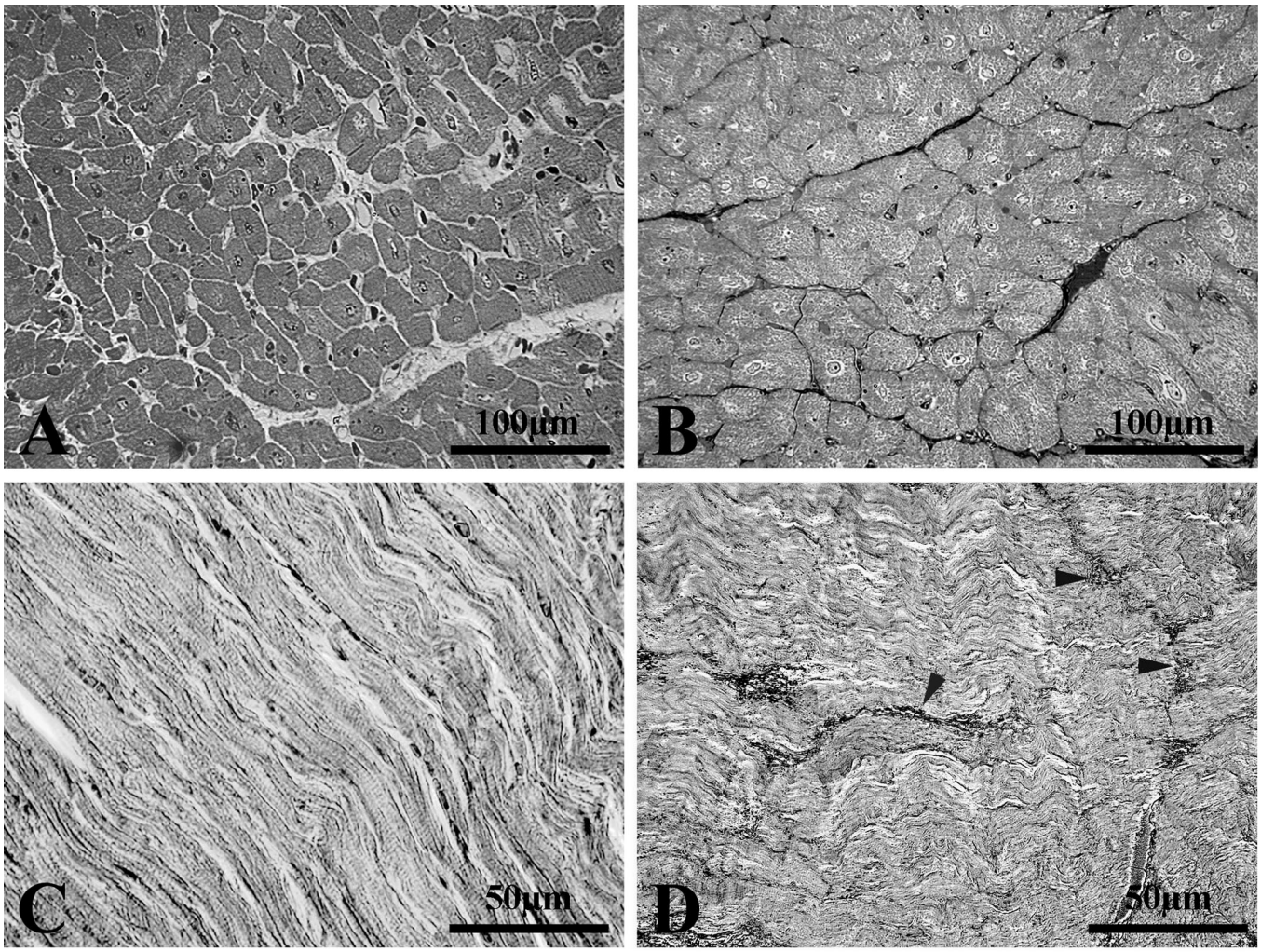

Table 2. Cardiomyocyte cross sections area (μm^2) (upper line) and myocardial fibrosis (bottom line) area ($\mu m^2/100\mu m^2$)

	C	6 h	24 h	48 h	96 h	168 h	2 m	3 m
a	225.31±32.69	249.20±32.87	266.60±33.21	280.05±51.31	425.32±56.47	492.04±49.82	447.60±32.92	773.84±75.87
b	0.74±0.16	1.47±0.38	1.27±0.34	1.24±0.20	1.56±0.20	1.36±0.30	1.35±0.35	1.36±0.31

Fig. 3. LM micrograph showing myocardial hypertrophy. Sham-operated (control) and 96h volume-overloaded cardiomyocytes **(A, B).** Collagen fibers in sham-operated (control) and 96 h volume-overloaded myocardium **(C and D).** Increased cardiomyocyte cross-sectional areas and foci of interstitial fibrosis are shown. Toluidine blue-stained cardiomyocytes **(A, B)**. Modified Masson's trichrome-stained myocardium **(C, D)**. **Table 2.** Morphometric evaluation of myocyte-cross sectional area (μm^2) **(a)** and of interstitial fibrosis ($\mu m^2/100\mu m^2$) **(b)** in sham-operated (control) and volume-overloaded myocardium. **a)** All data are statistically significant vs each group examined except for 48h vs 24h and 24 vs 48h. **b)** All data are statistically significant vs controls except for 6 h.

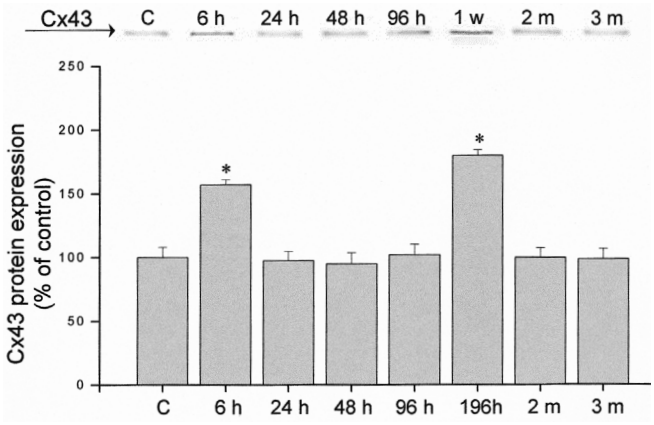

Fig. 4. Representative Western blot of Cx43 from control (C) and volume-overloaded myocardium. Bottom: Quantitative data. Each bar represents the mean ± S.D. of four different blots. Signals are quantified by densitometric analyses and are expressed as percentage of control values. Asterisk: significant differences ($p<0.05$) vs controls.

Table 2). In particular, cardiomyocyte hypertrophy started to be evident 96 h after surgery, and it gradually increased reaching its maximum values at 3 months, whereas myocardial interstitial fibrosis developed soon after the induction of the increased ventricular workload and remained unchanged during the whole experimental time.

Cx43 western blot analyses

To evaluate whether myocardial remodeling after the induction of volume overloading was associated with alterations in the levels of Cx43 gap-junction protein, Western blot analysis was carried out in all the myocardial samples. The immunochemical detection of this protein using moAb against Cx43 revealed a single band at the expected position (Fig. 4). The densitometric quantification of the bands revealed that there was a

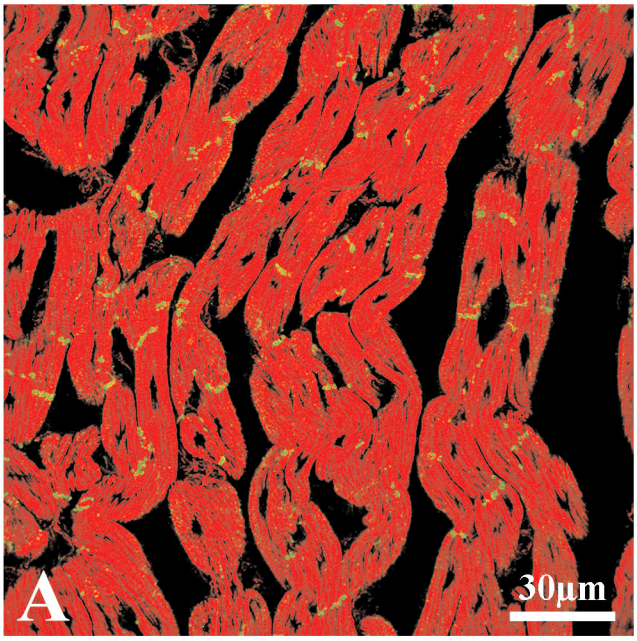

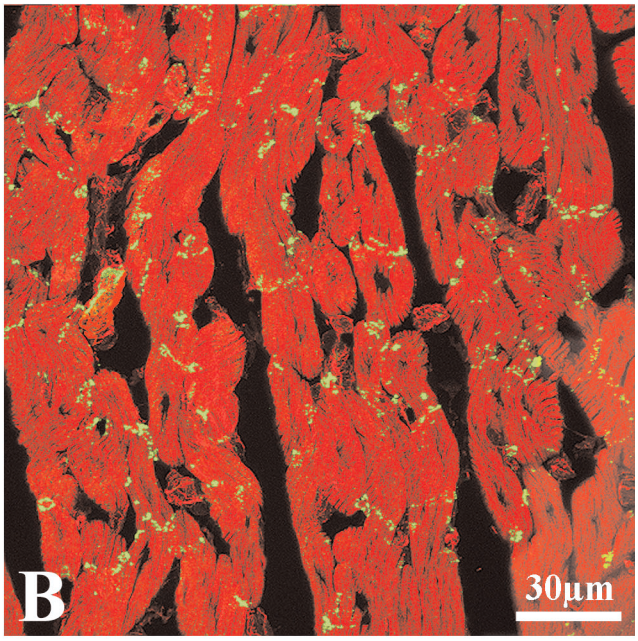

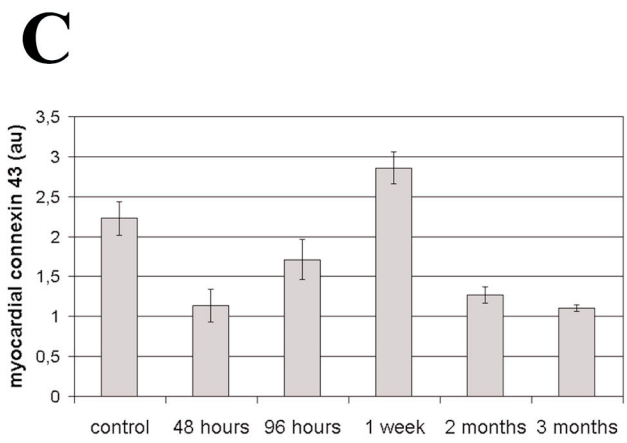

Fig. 5. Confocal fluorescence microscopy of anti-Cx43 immunostaining in the left ventricle of control **(A)** and 168 h **(B)** volume-overloaded myocardium. The green staining is highly localized in the intercellular appositional areas in the pattern of gap-junctions and intercalated disks in the control as well as volume-overloaded myocardium. **B.** A remarkable increase in Cx43 immunostaining with respect to that of controls is clearly visible. The images are the result of a projection of 15 optical sections. **C.** Quantitative confocal analyses of Cx43 in control and volume-overloaded myocardium. The proportion of the tissue area occupied by gap-junction Cx43 protein was calculated as the ratio between the number of pixels exceeding the threshold and the number of pixels representing the whole tissue area.

consistent increase in the expression of Cx43 in the myocardium within the first 6 h from surgery (+57%) as well as 168 h from surgery, when it reached its maximum value (+79%). The initial increase in the protein levels was followed by a significant drop in the expression of the gap-junction protein that peacked at 48 hrs, returning to the basal levels approximately at 96 h. The levels of this protein remained practically unchanged with respect to those of basal conditions during chronic myocardial hypertrophy (2-3 months from surgery).

Connexin43 confocal immunofluorescence analyses

To further analyze changes in Cx43 expression, myocardial samples from sham-operated and volume-overloaded animals were immunostained using Cx43 antibodies and analyzed by confocal microscopy. In the control myocardium, the immunoreactive signals showed a relatively uniform distribution and appeared as aggregates of punctuate fluorescent domains concentrated at points of intercellular appositions, in a pattern consistent with the distribution of gap-junctions and intercalated disks. Double staining of Cx43 (green) and actin (red) confirmed the presence of the gap-junctional protein in the cell-to-cell contact regions (Fig. 5A). It was evident from the inspection of the sections from volume-overloaded samples that the tissue distribution of the gap-junction protein did not differ substantially from controls, suggesting that no dispersion of the gap-junctional protein occurred during acute as well as chronic ventricular overloading. Moreover, the amount of Cx43 signals appeared particularly enhanced in the myocardium subjected to 168 h of increased workload (Fig. 5B). The quantitative analysis of digitized confocal images confirmed the visual findings and showed that a significant increase in the amount of the immunoreactive Cx43 signal, normalized to actin filaments, occurred in cardiomyocytes subjected to 168 hours of LV overloading (Fig.6). In contrast, the proportion of Cx43 label was significantly reduced compared with controls during the period of tissue damage (48 and 96 h), as well as in the advanced periods of the hypertrophic growth (2-3 month).

To identify potential mechanisms responsible for the accumulation of Cx43 protein during the initial phases of myocardial remodeling, we analyzed, by a semi quantitative RT-PCR technique, the levels of its specific mRNA. By this technique it was possible to reveal a remarkable increase in the expression of Cx43 mRNA in the myocardium subjected to 7 days of volume-overloading, whereas no changes in the levels of Cx43 mRNA were observed in any other time point considered (Fig. 6).

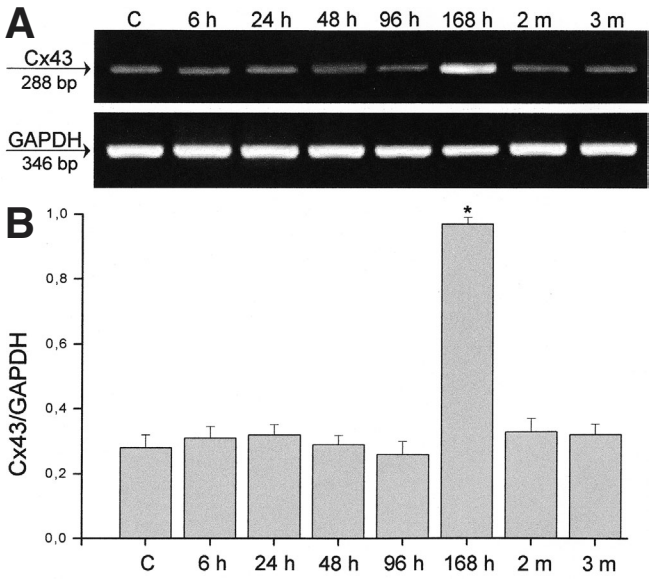

Fig. 6. Total RNA was extracted for cDNA synthesis and Cx43 mRNA was evaluated by a semiquantitative RT-PCR assay (see "Experimental Procedures" for details); the experiments were done in triplicate. **A.** An example of a RT-PCR gel showing Cx43 mRNA levels at different times (from 6 hours up to 3 months) after volume overload; lane C is from normal control. **B.** Graphic representation of Cx43 mRNA levels evaluated by a semiquantitative RT-PCR technique. Amplification products were run on an agarose gel and the ethidium bromide-stained bands were quantitated by densitometric analysis. Each histogram represents the mean ± S.E. of three values of Cx43 amplification products normalized to the corresponding GAPDH values.

Discussion

The results of the present study demonstrate that pig hearts subjected to LV volume overloading by the creation of an abdominal aorto-cava shunt, undergo a period of intense tissue remodeling characterized by an initial phase of myocardial alterations and damage (from 6 up to 48 h) associated with functional abnormalities, followed by the development of a compensatory hypertrophic response (from 96 h to 3 m). In fact, the hypertrophic growth, which at the morphological level was characterized by the expansion of cardiomyocyte myofilaments and by a concurrent proliferation of interstitial fibroblasts and collagen deposition, was able to counteract the increased load and to maintain a normal cardiac performance for the whole period of the experimentation.

The remodeling period was associated with dynamic changes in the expression of ventricular Cx43 gap-junction protein. Connexin 43 is a member, together with Cx45, Cx40, Cx37, of the connexin family of gap junction proteins of the heart (Kostin et al.,1999; Saffitz et al., 2000b). It represents the predominant gap-junction protein of the working ventricular myocardium, where it is essential for maintaining electrical stability among cardiomyocytes (Guerrero et al., 1997; Saffitz, 1997; Lo, 2000). Cx43 protein, in fact, forms hexameric assemblies surrounding a central pore within the membrane of adjacent cardiomyocytes (Yeager, 1998) and the fusion of two adjacent pores at the intercalated

discs results in the formation of densely packed intercellular channels directly connecting the cytoplasmic compartments of cardiomyocytes. Moreover, loss of Cx43 expression has been shown to be a key anatomic substrate of arrhythmias in chronically hypertrophied myocardium (Wang and Gerdes, 1999; Jongsma and Wilders, 2000). Of interest, we have shown in the present study that there was a marked increase in the levels of Cx43 protein in the earliest phases (6 h) and after 168 h of volume overloading, whereas the amount of Cx43 decreased both during the period of tissue damage (24 and 48 h) as well as during chronic volume overloading. Although several reports in the literature have shown down-regulation of Cx43 protein levels in chronically hypertrophied hearts, the data concerning its up-regulation during early stages of ventricular remodeling is, to our knowledge, the first "in vivo" experimental evidence to suggest a role for this protein in the adaptive processes of the heart to acute increased ventricular overload. Similar conclusions have been previously speculated by "in vitro" experiments, showing that an increase in Cx43 expression and in the intercellular propagation velocity occur in cultured neonatal rat cardiomyocytes exposed for 24 h to early mediators of heart hypertrophy, such as dibutyryl cAMP, AngII, ET-1, or alternatively to short-term pulsatile stretches (Darrow et al., 1996; Dodge et al.,1998; Zhuang et al., 2000; Polontchouk et al., 2002). Thus, the results of the present study combined with the above reported observations, suggest that myocardial Cx43 gap-junction protein and intercellular electrical coupling may be up-regulated early after the application of the increased workload, with the exception of the period of maximal tissue damage, in order to face the new working conditions and improve cardiac functions.

The maintenance of a normal cardiac performance despite the decrease in Cx43 protein expression at the gap-junctions during the chronic stages of myocardial hypertrophy may be explained taking into consideration that such a reduction may not be sufficient to cause abnormalities in the electrical coupling among cardiomyocytes, at least in our experimental model. Beside reduction in Cx43 protein expression, one of the most commonly found alterations in diseased hypertrophic myocardium is the redistribution of gap-junction plaques from end-to-end to lateral cell borders (Sepp et al., 1996; Uzzaman et al., 2000; van Veen et al., 2001). In our samples, in contrast, the immunoreactive signal appeared to be exclusively localized to gap-junctions. Moreover, it is likely that other compensative mechanisms, including the hypertrophic response of cardiomyocytes and the improvement in the cardiac intracellular calcium handling may be relevant in the latest stage of compensatory cardiac hypertrophy. Indeed, we have recently demonstrated, using the same experimental model of pig heart hypertrophy, that calcium-regulating proteins may be up-regulated by prolonged (2-3 month) LV overloading and, in particular, that increased expression and activity of acyl-phosphatase, with its stimulatory effects on SR calcium uptake, contributes to enhance the contractile reservoirs in cardiomyocytes in these experimental conditions (Nediani et al., 2002).

It is well accepted that gap-junction proteins are remarkably dynamic molecules with a half life of about 1.5 hours in the adult heart (Saffitz et al., 2000a,b) and that their remodeling is a very complex process involving not only changes in connexin synthesis but also in connexin assembly into intercellular channels and connexin degradation (Beardslee et al., 1998). In search for possible mechanisms involved in the accumulation of Cx43 protein during acute LV overloading, we analyzed the expression of its specific mRNA. We found that the increase in CX43 levels reflected increased Cx43 mRNA expression at 168 h from surgery. Since no variation in mRNA levels were found in the very early phases of our experimentation (6 h), it is possible that the short-term effects on Cx43 protein levels may be due to a decrease in the turnover of the protein and/or to other mechanisms acting at the post-transcription level. Indeed, the possibility that increased Cx43 protein expression may not involve changes in its mRNA has also been recently demonstrated by the identification of a functional internal ribosomal entry site (IRES) in the 5'-UTR Cx43 mRNA (Holcik et al., 2000). This peculiar site provides an additional translation initiation independently from that assured by the cap structure in Cx43 mRNA, which may strongly increase Cx43 protein synthesis rate. To further support this hypothesis, it has been recently demonstrated that a switch to IRES-mediated translational control occurs in response to mechanical stretching in cardiac transfected cell lines (Schiavi et al., 1999).

In conclusion, although the mechanisms undergoing myocardial remodeling induced by LV volume overloading are certainly highly complex, the results of the present study are in favor for an up-regulation of Cx43 protein expression as a part of the immediate adaptive response of the heart to increased workload. The increased levels of Cx43 at sites of cell-to-cell contacts may reflect activation of different regulatory mechanisms acting at both transcriptional and post-transcriptional level.

Acknowledgements. This work was supported by the Ministero della Ricerca Scientifica e Tecnologica (MURST 60%) to L. Formigli, L. Ibba-Manneschi, S. Zecchi-Orlandini.

References

Anversa P. and Capasso J.M. (1991). Cardiac hypertrophy and ventricular remodeling. Lab. Invest. 64, 441-445.

Baker K.M., Chernin M.I., Wixon S.K. and Aceto J.F. (1990). Renin-angiotensin system involvement in pressure-overload cardiac hypertrophy in rats. Am. J. Physiol. (Circ. Physiol.) 259, H324-H332.

Beardslee M.A., Laing J.G., Beyer E.C. and Safftz J.E. (1998). Rapid turnover of connexin43 in the adult rat heart. Circ. Res. 83, 629-635.

Beardslee M.A., Lerner D.L., Tadros P.N., Laing J.G. Beyer E.C., Yamada K.A., Kebler A.G., Schulssler R.B. and Saffitz J.E. (2000).

Dephosphorilation and intracellular redistribution of ventricular connexin43 and electrical uncoupling induced by ischemia. Circ. Res. 87, 656-662.

Chien K.R. (1999). Stress pathways and heart failure. Cell 98, 555-558.

Darrow B.J, Fast V.G., Klèber A.G., Beyer E.C. and Saffitz J.E. (1996). Functional and structural assessment of intercellular communication. Increased conduction velocity and enhanced connexin expression in Dibutyrryl c-AMP treated cultured cardiac cardiomyocites. Circ. Res. 79, 174-183.

Devereux R.B. and Reichek N. (1997). Echocardiographic determination of the left ventricle mass in man; validation of the method. Circulation 55, 613-618.

Dodge S.M., Beardslee M.A., Darrow B.J., Green K.G., Beyer E.C. and Saffitz J.E. (1998). Effects of angiotensin II on expression of the gap junctions channel protein connexin43 in neonatal rat ventricular myocytes. J. Am. Coll. Cardiol. 32, 800-807.

Dupont E., Matsushita T., Kaba R.A., Vozzi C., Coppen S.R., Khan N., Kaprielian R., Yacoub M.H. and Severs N.J. (2001). Altered connexin expression in human congestive heart failure. J. Mol. Cell Cardiol. 33, 359-371.

Emdad L., Uzzaman M., Takagishi Y., Honjo H., Uchida T., Severs N.J., Kodama I. and Murata Y. (2001). Gap junction remodeling in hypertrophied left ventricles of aortic-banded rats: prevention by angiotensin II type receptor blockade. J. Mol. Cell Cardiol. 33, 219-231.

Guerrero P.A., Schuessler R.B., Davis L.M., Beyer E..C., Johnson C.M., Yamada K.A. and Saffitz J.E. (1997). Slow ventricular conduction in mice heterozygous for a connexin-43 null mutation. J. Clin. Invest. 99, 1991-1998.

Holcik M., Sonenberg N. and Korneluk K.G. (2000). Internal ribosome initiation translation and the control of cell death. Trends Genet. 16, 469-473.

Jongsma H.J. and Wilders R. (2000). Gap junctions in cardiovascular disease. Circ. Res. 86, 1193-1197.

Kostin S., Hein S., Bauer E.P. and Schaper J. (1999). Spatiotemporal development and distribution of intercellular junctions in adult rat cardiomyocytes in culture. Circ. Res. 85, 154-167.

Lo C.W. (2000). Role of gap junctions in cardiac conduction and development. Insights from the connexin knockout mice. Circ. Res. 87, 346-348.

Mercadier J.J. Lomprè A-M. and Wisnewsky C. (1981). Myosin isoenzymic changes in several models of rat cardiac hypertrophy. Circ. Res. 49, 525-532.

Minamisawa S., Hoshijima M., Chu G., Ward C.A., Frank K., Gu Y., Martone M.E., Wang Y., Ross J., Kranias E.G., Giles W.R. and Chien K.R. (1999). Chronic phospholamban-sarcoplasmic reticulum calcium ATPase interaction is the critical calcium cycling defect in dilated cardiomyopathy. Cell 99, 313-322.

Modesti P.A., Vanni S., Bertolozzi I., Cecioni I., Polidori G., Paniccia R., Bandinelli B., Perna A.M., Liguori P., Boddi M., Galanti G. and Neri Serneri G.G. (2000). Early sequences of cardiac adaptations and growth factor formation in pressure- and volume-overload hypertrophy. Am. J. Physiol. (Heart Circ. Physiol.) 279, H976-H985.

Molkentin J.D. (2000). Calcineurin and beyond. Cardiac hypertrophic signaling. Circ. Res. 87, 731-738.

Nediani C., Formigli L., Perna A.M., Pacini A., Modesti P.A., Vanni S., Ibba Manneschi L., Zecchi Orlandini S., Fiorillo C., Cecchi C., Liguori P., Fratini G. and Nassi P. (2002). Biochemical changes and their relationship with morphological and functional findings in pig heart subjected to lasting volume-overload: a possible role of acylphosphatase in the regulation of sarcoplasmic reticulum calcium pump. Basic Res. Cardiol. (in press).

Neri Serneri G.G., Cecioni I., Vanni S., Paniccia R., Bandinelli B., Vetere A., Janming X., Bertolozzi I., Boddi M., Lisi G.F., Sani G. and Modesti P.A. (2000). Selective up-regulation of cardiac endothelin system in patients with ischemic but not idiopathic dilated cardiomyopathy. Circ. Res. 86, 377-385.

Peters N.S. (1996). New insights into myocardial arrhythmogenesis: distribution of gap-junctional coupling in normal, ischaemic and hypertrophied human hearts. Clin. Sci. (Colch). 90, 447-452.

Peters N.S., Green C.R., Poole-Wilson P.A. and Severs N.J. (1993). Reduced content of connexin43 gap junctions in ventricular myocardium from hypertrophied and ischemic human hearts. Circulation 88, 864-875.

Polontchouk L., Ebelt B.,Jackels M. and Dhein S. (2002). Chronic effects of endothelin 1 and angiotensinII on gap junctions and intercellular communication in cardiac cells. FASEB J 16, 87-89.

Saffitz J.E. (1997). Gap-junctions: functional effects of molecular structure and tissue distribution. Adv. Exp. Med. Biol. 430, 219-301.

Saffitz J.E., Schuessler R.B. and Yamada K.A. (1999). Mechanisms of remodeling of gap junction distributions and the development of anatomic substrates of arrhythmias. Cardiovasc. Res. 42, 309-317.

Saffitz J.E., Green K.G., Kraft W..J., Schechtman K.B. and Yamada K.A. (2000a). Effects of diminished expression of connexin43 on gap junction number and size in ventricular myocardium. Am. J. Physiol. (Heart Circ. Physiol.) 278, H1662-H1670.

Saffitz J.E., Laing J.G. and Yamada K.A. (2000b). Connexin expression and turnover. Circ. Res. 86, 723-728.

Schiavi A., Hudder A. and Werner R. (1999). Connexin 43 mRNA contains a functional internal ribosome entry site. FEBS Lett. 464, 118-122.

Sepp R., Severs N.J. and Gourdie R.G. (1996). Altered patterns of cardiac intercellular junction distribution in hypertrohied cardiomyopathy. Heart 76, 412-417.

Severs N.J., Rothery S., Dupont E., Coppen S.R., Yeh H.I., Ko Y.S., Matsushita T., Kaba R. and Halliday D. (2001). Immunocytochemical analysis of connexin expression in the healthy and diseased cardiovascular system. Microsc. Res. Tech. 52, 301-322.

Uzzaman M., Honjo H., Takagishi Y., Emdad L., Magee A.I., Severs N.J. and Komada I. (2000). Remodeling of gap junctional coupling in hypertrophied right ventricles of rats with monocrotaline-induced pulmonary hypertension. Circ. Res. 86, 871-878.

Van Veen A.A., van Rijen H.V. and Opthof T. (2001). Cardiac gap junction channels: modulation of expression and channel properties. Cardiovasc. Res. 51, 217-229.

Wang X. and Gerdes A.M. (1999). Chronic pressure overload cardiac hypertrophy and failure in guinea pigs: III. Intercalated disc remodeling. J. Mol. Cell Cardiol. 31, 333-343.

Wijsman J.H., Jonker R.R., Keijzer R., van de Velde C.J.H., Cornellisse C.J. and van Dierendonck J.H. (1993). A new method to detect apoptosis in paraffin sections: In situ labeling of fragmented DNA. J. Histochem. Cytochem. 41, 7-12.

Yeager M. (1998). Structure of cardiac gap-junction intercellular channels. J. Struct. Biol. 121, 231-245.

Zhuang J., Yamada K.A., Saffitz J.E. and Klèber A.G. (2000). Pulsatile stretch remodels cell-to-cell communication in cultured myocytes. Circ. Res. 87, 316-322.

Accepted November 15, 200